Trapped electromagnetic modes in a waveguide with a small discontinuity

G. V. Stupakov and S. S. Kurennoy
Superconducting Super Collider Laboratory, 2550 Beckleymeade Avenue, Dallas, Texas 75237
(Received 23 June 1993)

We demonstrate that a small discontinuity (such as an enlargement or a hole) on a smooth waveguide can result in the appearance of trapped modes localized in the vicinity of the discontinuity. The frequencies of these modes lie slightly below the cutoff frequencies of the corresponding propagating modes in the waveguide. We find the distribution of the electromagnetic field in the modes and calculate their damping rate due to a finite conductivity of the walls. The contribution of the trapped modes to the longitudinal impedance is calculated.

PACS number(s): 41.75.−i, 41.20.−q

I. INTRODUCTION

Previous computer studies of the impedance of a cavity coupled to a beam pipe indicated that the longitudinal impedance of a small chamber enlargement exhibits sharp narrow peaks at frequencies close to the cutoff frequencies of the waveguide [1–3]. No theoretical explanation has been given for this phenomenon. Only recently Balbekov treated this effect in terms of equivalent circuits associated with a small enlargement, and calculated the parameters of the peaks [4].

In this paper, we want to demonstrate that from the point of view of electromagnetic theory these peaks can be attributed to trapped modes localized near a small discontinuity at a smooth waveguide. First, we show that a small axisymmetric enlargement on a waveguide creates localized transverse magnetic (TM) modes having the frequencies below the cutoff frequencies of the corresponding propagating modes. Having found the electromagnetic field distribution in those modes we are able to calculate their damping rates due to finite conductivity of the walls and to find a corresponding contribution to the longitudinal impedance. We also discuss requirements on the wall conductivity for these modes to exist.

Another important practical example of a beam-pipe discontinuity is a small pumping hole. The low-frequency impedance of a hole (at frequencies well below the cutoff frequency) has been studied in Refs. [5,6]. Calculation of the impedance at frequencies compared with or above the cutoff frequency requires knowledge of the eigenmodes of the waveguide with a hole. As a first step in this direction, we show that, similar to the case of the axisymmetric enlargement, a hole also creates localized modes. A physical mechanism responsible for appearance of the localized modes in both cases is the interaction of the induced magnetic moment of the discontinuity with a slowly propagating mode near the cutoff frequency.

The paper is organized as follows. In Sec. II we consider the case of an axisymmetric enlargement and develop a method based on the use of the Lorentz reciprocity theorem for evaluating the frequency of the trapped mode. In Sec. III, we apply this method to the case of a small hole in the wall, assuming that the hole size is much smaller than the pipe radius. Consideration in Secs. II and III is restricted to the case of axisymmetric TM modes only. In Sec. IV, we present the results for the nonaxisymmetric TM trapped modes for both the cases of the enlargement and of the hole. Section V is devoted to consideration of the trapped TE modes and Sec. VI summarizes our results.

II. AXISYMMETRIC ENLARGEMENT

In this section, we restrict our attention to an axisymmetric electromagnetic field having nonzero E_z component, because only this field contributes to the longitudinal impedance. In a cylindrical waveguide with perfectly conducting walls, such a field is represented by axisymmetric TM modes with the following components of the electromagnetic field [we omit the factor $\exp(-i\omega t)$ throughout this paper]:

$$\begin{aligned} E_z^{(m)} &= \frac{\mu_m^2}{b^2} J_0\left(\frac{\mu_m r}{b}\right) \exp(\mp\kappa_m z) \,, \\ E_r^{(m)} &= \pm\frac{\mu_m \kappa_m}{b} J_1\left(\frac{\mu_m r}{b}\right) \exp(\mp\kappa_m z) \,, \\ Z_0 H_\theta^{(m)} &= -\frac{i\omega\mu_m}{cb} J_1\left(\frac{\mu_m r}{b}\right) \exp(\mp\kappa_m z) \,, \end{aligned} \tag{1}$$

where $Z_0 = \sqrt{\mu_0/\varepsilon_0} = 120\pi\ \Omega$ is the impedance of free space, J_0 and J_1 are the Bessel functions of the zeroth and first order, μ_m is the mth root of J_0, $m = 1, 2, \ldots$, and b is the radius of the waveguide. In Eqs. (1) $\kappa_m = \sqrt{\omega_m^2 - \omega^2}/c$, where $\omega_m = \mu_m c/b$ is the cutoff frequency, and we assume $\omega < \omega_m$ so that κ_m is a positive real number, and the upper (lower) sign corresponds to waves "propagating" in the positive (negative) z direction.

We will assume that the characteristic dimension of the discontinuity is much smaller than the pipe radius b (see Fig. 1). As a consequence, the frequency of the trapped mode Ω_m, $\Omega_m < \omega_m$, will be very close to the cutoff frequency ω_m. Defining the wave vector $k_m = \sqrt{\omega_m^2 - \Omega_m^2}/c$ associated with Ω_m, one can write down asymptotic expressions for the field of the mth trapped mode $\mathcal{E}_z^{(m)}$, $\mathcal{E}_r^{(m)}$, and $\mathcal{H}_\theta^{(m)}$ choosing the signs in Eqs. (1)

1063-651X/94/49(1)/794(6)/$06.00

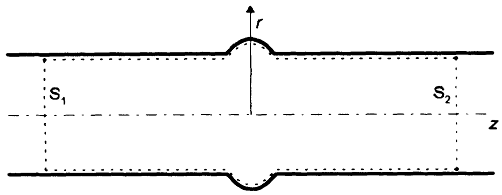

FIG. 1. Cylindrical waveguide with an enlargement. The dotted line shows the integration surface in the Lorentz reciprocity theorem.

so that the field goes to zero when $|z| \to \infty$:

$$\begin{aligned} \mathcal{E}_z^{(m)} &= \frac{\mu_m^2}{b^2} J_0\left(\frac{\mu_m r}{b}\right) \exp(-k_m|z|) \ , \\ \mathcal{E}_r^{(m)} &= \operatorname{sgn}(z) \frac{\mu_m k_m}{b} J_1\left(\frac{\mu_m r}{b}\right) \exp(-k_m|z|) \ , \\ Z_0 \mathcal{H}_\theta^{(m)} &= -\frac{i\omega\mu_m}{cb} J_1\left(\frac{\mu_m r}{b}\right) \exp(-k_m|z|) \ . \end{aligned} \quad (2)$$

Strictly speaking, Eqs. (2) are valid in the limit $|z| \gg b$; for $|z| \sim b$ one has to add terms with $m' > m$ on the right hand side of Eqs. (2), which exponentially decay on the distance of the order of b. Our theory is based on the assumption that

$$k_m b \ll 1 \ , \quad (3)$$

in other words, the trapped mode is spread along the axis of the pipe over the distance $k_m^{-1} \gg b$. The asymptotic dependencies given by Eqs. (2) as functions of z (for a given r) are shown in Fig. 2. Both $\mathcal{E}_z^{(m)}$ and $\mathcal{H}_\theta^{(m)}$ turn out to be continuous at $z = 0$. Noting that the characteristic scale on which they change is large compared with b, we can conclude that in the region where Eqs. (2) are not formally applicable one can still use the first and the last of them to represent the components $\mathcal{E}_z^{(m)}$ and $\mathcal{H}_\theta^{(m)}$ (see Fig. 2). The error arising from using these equations in the region $|z| < b$ is small, of the order of $k_m b$. As for the $\mathcal{E}_r^{(m)}$, it departs appreciably from its asymptotic form in this region (see Fig. 2). However, as this component is relatively small ($\mathcal{E}_r^{(m)} \sim k_m b \mathcal{E}_z^{(m)}$), it will not be needed in what follows.

To find the eigenfrequency of the trapped mode we will utilize the Lorentz reciprocity principle, which states that for any two solutions of Maxwell's equations without sources the following equality holds [7]:

$$\int dS \mathbf{n}(\mathbf{E}_1 \times \mathbf{H}_2 - \mathbf{E}_2 \times \mathbf{H}_1) = \mathbf{0} \ , \quad (4)$$

where the integration runs over a closed surface S consisting of the surface of the waveguide wall and two plane end surfaces in the xy plane, S_1 and S_2, as shown in Fig. 1. The unit vector $\mathbf{n}$ in Eq. (4) is normal to the surface S and directed outward. We now let $\mathbf{E}_1, \mathbf{H}_1$ be the field of the trapped mode, and $\mathbf{E}_2, \mathbf{H}_2$ be the TM mode having the frequency Ω_m of the trapped mode and exponentially decaying proportional to $\exp(-k_m z)$ in the positive direction. This casts Eq. (4) into

$$\int dS \mathbf{n} \cdot (\boldsymbol{\mathcal{E}}^{(m)} \times \mathbf{H}^{(m)} - \mathbf{E}^{(m)} \times \boldsymbol{\mathcal{H}}^{(m)}) = 0 \ . \quad (5)$$

Moving the surface S_2 far enough from the discontinuity, we can make its contribution to the integral (5) vanishing because both fields exponentially decay when $z \to \infty$. As for the surface S_1, we choose to place it in the region where one can use the asymptotic expansion (2) for the trapped mode. A simple integration over S_1 yields

$$-\frac{2\pi i \Omega_m \mu_m^2 k_m}{Z_0 c} J_1^2(\mu_m) \ . \quad (6)$$

Turning to the integration over the wall surface, note first that due to the perfect conductivity of the wall we have the boundary condition $\boldsymbol{\mathcal{E}}^{(m)} \times \mathbf{n} = \mathbf{0}$, which makes the first term in Eq. (5) vanish. The remaining term also vanishes at the cylindrical part of the waveguide, $r = b$, because there $\mathbf{E}^{(m)} \times \mathbf{n} = \mathbf{0}$. Hence the only contribution from the wall surface comes from the region of the waveguide enlargement and has the form $-\int dS \mathbf{n} \cdot \mathbf{E}^{(m)} \times \boldsymbol{\mathcal{H}}^{(m)}$. As was noted above, the magnetic field in the trapped mode with desired accuracy is given by the asymptotic formula (2) (where one has to put $r = b$ and $z = 0$ because of the assumed smallness of the enlargement). For the z component of $\mathbf{E}^{(m)}$ we use the first of Eqs. (1) with $z = 0$ and expand the Bessel function in the small ratio $(r - b)/b$, namely, $J_0(\mu_m r/b) \simeq -\mu_m J_1(\mu_m)(r - b)/b$. We also neglect $E_r^{(m)}$ as a small quantity. Performing the integration one finds

$$\frac{2\pi i \Omega_m \mu_m^4 A}{Z_0 c b^3} J_1^2(\mu_m) \ , \quad (7)$$

where A is the area of the cross section of the enlargement in the rz plane. Note that A enters Eq. (7) with its sign; e.g., for an iris that protrudes into the pipe, A would have a negative sign.

Combining Eqs. (6) and (7) gives an equation for k_m,

$$k_m = \frac{\mu_m^2 A}{b^3} \ , \quad (8)$$

which can easily be solved for the frequency Ω_m,

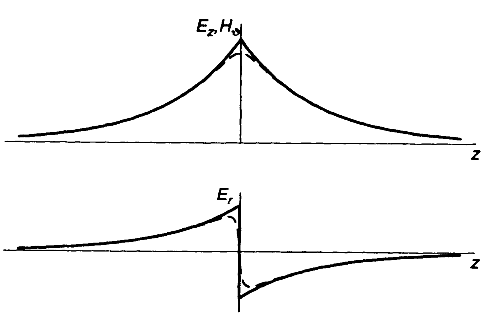

FIG. 2. The fields in a trapped mode. Solid lines show asymptotics given by Eqs. (2); dashed lines are for the exact solutions (qualitatively).

$$\Omega_m = \omega_m \left[1 - \frac{\mu_m^2}{2}\left(\frac{A}{b^2}\right)^2\right] . \tag{9}$$

As mentioned above, in the case of an iris $A < 0$ and Eq. (8) cannot be satisfied because its left and right hand sides have different signs. This means that the trapped mode arises only if the integrated waveguide cross section increases due to the presence of the discontinuity.

To check our analytical results, namely, Eq. (9), we have carried out numerical computations of the lowest eigenfrequency in a long cylindrical resonator with a small pillbox by means of the code SUPERFISH [8]. The waveguide cutoff frequency ω_1 corresponds to the eigenfrequency of the E_{010} mode in the smooth (without pillbox) resonator with the same radius. The presence of a small pillbox shifts this eigenfrequency down. To exclude the influence of the side walls and make possible the comparison with the theory, one has to choose length L of the resonator to be large, $L \gg k_1^{-1} = b^3/(\mu_1^2 A)$. It means that the resonator length is larger than that of the region where the trapped mode is localized. We have used $b = 2$ cm, $A \simeq 0.1 - 0.5$ cm^2, and L from 30 cm to 100 cm to satisfy the inequality above. In Fig. 3 the frequency shift is plotted versus the area of the pillbox cross section. It is seen that our numerical and analytical results are in good agreement. Figure 4 shows the electric field lines for one of the resonator eigenmodes that corresponds to the trapped mode in the waveguide with the same small pillbox cavity.

The calculations above were performed for a perfectly conducting pipe. Let us assume now a finite, though large, conductivity of the walls. As a result of energy dissipation in the walls, the trapped mode frequency acquires a negative imaginary part, $\Omega_m \to \Omega_m - i\gamma_m$, $\gamma_m > 0$. The damping rate γ_m can be easily computed using the given field profile [Eqs. (2)] as half of the energy absorbed in the walls per unit time divided by the total energy in the mode [9]. This gives the following result:

$$\gamma_m = \frac{\omega_m \delta}{2b} , \tag{10}$$

where $\delta = \sqrt{2/(\mu_0 \sigma \omega_m)}$ is the skin depth in the pipe wall whose conductivity is σ.

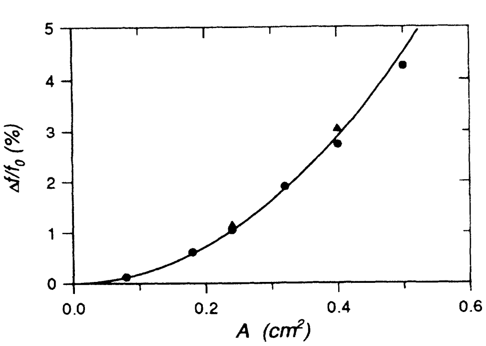

FIG. 3. Frequency shift versus the pillbox area ($\Delta f = f_0 - f$, where f_0 is the cutoff frequency and f is the frequency of the trapped mode). The solid line corresponds to Eq. (9).

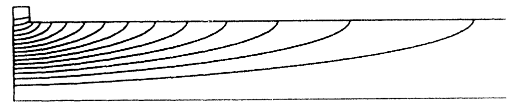

FIG. 4. Electric field lines in a trapped mode.

At this point, we have to note that the damping with the decrement γ_m can also be treated as a frequency spread $\sim \gamma_m$ associated with the trapped mode. Should this spread be compared to or larger than the gap between Ω_m and the cutoff frequency of the mode ω_m, the frequency content of the mode would include harmonics above the cutoff frequency. These harmonics are able to propagate along the pipe, destroying the initially trapped mode. Hence we expect that the mode should disappear when γ_m becomes comparable to or greater than $(\omega_m - \Omega_m)$. A more detailed study should predict an exact ratio of $\gamma_m/(\omega_m - \Omega_m)$, above which the trapped mode ceases to exist.

Calculating the longitudinal impedance as that of a cavity with given eigenmodes (for example, see Ref. [10]), one can find the longitudinal impedance produced by the trapped mode:

$$Z_m(\omega) = \frac{2i\Omega_m \gamma_m R_m}{\omega^2 - (\Omega_m - i\gamma_m)^2} , \tag{11}$$

where the shunt impedance R_m is

$$R_m = \frac{4 Z_0 \mu_m A^3}{\pi \delta b^5 J_1^2(\mu_m)} . \tag{12}$$

We have to emphasize here that Eq. (11) describes only the contribution of the peak to the longitudinal impedance; the propagating modes in the pipe are not included. It is important that in the limit of perfect conductivity, $\delta \to 0$, Eq. (11) gives an infinitely high and narrow peak. This kind of resonance near cutoff frequencies of the waveguide with a small pillbox and perfectly conducting walls has been observed in Ref. [1] in numerical computations using the field-matching technique. An integral equation method [2] has shown similar resonances slightly below cutoffs, with the same dependence of R_m on the wall conductivity σ ($R_m \propto \delta^{-1} \propto \sqrt{\sigma}$) as predicted by Eq. (12). Finally, in a recent paper [4] based on the equivalent-circuit method, the equations for the resonant frequency and impedance have been derived that agree with our Eq. (9) and with Eq. (12) within a numerical factor.

III. TRAPPED MODE DUE TO A HOLE

As another application of the method developed in the preceding section we will show here that a small hole in the pipe wall also creates localized axisymmetric TM modes. We assume that the dimensions of the hole are much smaller than the pipe radius. Again, we begin from consideration of a perfectly conducting waveguide.

Most of the derivation of the preceding section, including Eqs. (1)–(5), is applicable to the case of the hole without any changes. The integration in Eq. (5) now goes over the cylindrical surface $r = b$ bounded by the end surfaces S_1 and S_2. The contribution from the end surfaces is the same as given by Eq. (6); however, instead of Eq. (7) one has to perform the integration in Eq. (5) over the hole.

Considering the integrand in Eq. (5) at the hole, note that the first term vanishes because $\mathbf{E}^{(m)} \times \mathbf{n} = \mathbf{0}$ at $r = b$. Hence the integral reduces to $\int dS\mathbf{n} \cdot \mathcal{E}^{(m)} \times \mathbf{H}^{(m)}$. The magnetic field $\mathbf{H}^{(m)}$ has the azimuthal component, $\mathbf{n}$ is directed along the radius, and the integral can be written in the following form: $H_\theta^{(m)} \int dS\mathcal{E}_z^{(m)}$. (We put $H_\theta^{(m)}$ in front of the integral, neglecting its variation over the hole.) The distribution of the tangential electric field in the hole can be related to the surface density of the magnetic current K_θ, introduced formally in the problem of diffraction by small holes [11], $\mathcal{E}_z^{(m)} = -K_\theta^{(m)}/2$. This allows one to reduce the integral to

$$-\frac{1}{2} H_\theta^{(m)} \int dS K_\theta^{(m)} . \tag{13}$$

Now, noting that $\int dSK_\theta^{(m)} = -i\omega\mu_0 M_\theta$, where M_θ is the θ component of the induced magnetic moment of the hole, and introducing the magnetic susceptibility of the hole α_θ as $M_\theta = \alpha_\theta H_\theta$, one finds that the expression

$$\frac{i\Omega_m^2 \mu_m^2 J_1^2(\mu_m)\alpha_\theta}{2Z_0 c^3 b^2} \tag{14}$$

should substitute Eq. (7) in the case of the hole. Comparing Eq. (14) with Eq. (7), we conclude that all of the results of Sec. II remain valid for the hole if we put the quantity $\alpha_\theta/(4\pi b)$ in Eqs. (7)–(12) instead of the area of the enlargement cross section A:

$$A \to \frac{\alpha_\theta}{4\pi b} . \tag{15}$$

It is interesting that the area A can also be treated as related to the magnetic susceptibility of the enlargement. Indeed, if we equate the magnetic energy in the enlargement $\pi\mu_0 bAH_\theta^2$ to the energy of a magnetic moment M immersed into magnetic field H_θ, $\mu_0 MH_\theta/2$, we find that the magnetic moment of the enlargement is $M = 2\pi bAH_\theta$. This gives for the susceptibility of the enlargement $2\pi bA$, which agrees with the relation (15) within a factor of 2.

According to Eqs. (9) and (15), the frequency of the trapped mode created by the hole is

$$\Omega_m = \omega_m \left[1 - \frac{\mu_m^2}{2}\left(\frac{\alpha_\theta}{4\pi b^3}\right)^2\right] . \tag{16}$$

Magnetic susceptibility of elliptic holes can be found in Ref. [7]. For a round hole, $\alpha_\theta = 8a^3/3$, and the frequency gap $(\omega_m - \Omega_m)$ is proportional to $(a/b)^6$. The same scaling law is also valid for other hole shapes if a is understood as a characteristic dimension of the hole.

Radiation through the hole in the outer space creates another channel of damping of the trapped mode in addition to the damping due to a finite conductivity of the walls. This damping can be estimated as follows. Assume that the radiated field propagates freely away from the waveguide, and use for the estimate of the radiated energy the formula $Z_0(\omega/c)^4 M_\theta^2/24\pi$ for the energy loss of an oscillating magnetic dipole in the empty space. (We have included an additional factor of 1/2 in this formula, counting only the radiation that goes outside the waveguide.) Dividing this quantity by the double total energy in the mode we can find the damping rate $\gamma_{\rm rad}$ in the following form:

$$\gamma_{\rm rad} = \frac{\omega_m \mu_m^3 \alpha_\theta^2 k_m}{3b^5} . \tag{17}$$

In addition to the radiation into the outer space the trapped mode also loses energy via coupling effects by inducing propagating modes having cutoff frequency below Ω_m. This coupling can be considered as radiation into the waveguide with a damping rate which, within a numerical factor, can also be estimated as that given by Eq. (17). Comparing $\gamma_{\rm rad}$ with the frequency of the trapped mode we find that

$$\frac{\gamma_{\rm rad}}{\omega_m - \Omega_m} \sim \mu_m k_m b \sim \left(\frac{\mu_m a}{b}\right)^3 , \tag{18}$$

which reads that for small m the radiation damping is small compared with the frequency gap between the mode and cutoff frequency. Hence the radiation does not destroy the trapped mode due to the broadening of the resonant frequency, as described in the preceding section.

IV. HIGHER-ORDER TM MODES

In the previous sections, we presented a detailed derivation of the axisymmetric trapped modes. The same method can be applied without any changes to the nonaxisymmetric TM modes having the azimuthal dependence on θ as sine or cosine of $n\theta$. Below we give without derivation the field distribution and equations for the frequency of these modes.

The electromagnetic field in the trapped mode is now given by the following expressions:

$$\begin{aligned} \mathcal{E}_z^{(n,m)} &= \frac{\mu_{n,m}^2}{b^2} J_n\left(\frac{\mu_{n,m} r}{b}\right) \\ &\quad \times \exp(-k_{n,m}|z|)\sin(n\theta + \phi) , \\ Z_0\mathcal{H}_\theta^{(n,m)} &= \frac{i\omega\mu_{n,m}}{cb} J_n'\left(\frac{\mu_{n,m} r}{b}\right) \\ &\quad \times \exp(-k_{n,m}|z|)\sin(n\theta + \phi) , \\ Z_0\mathcal{H}_r^{(n,m)} &= -\frac{i\omega n}{cr} J_n'\left(\frac{\mu_{n,m} r}{b}\right) \\ &\quad \times \exp(-k_{n,m}|z|)\cos(n\theta + \phi) , \end{aligned} \tag{19}$$

where the new index n is associated with azimuthal variation of the field, $\mu_{n,m}$ is the mth root of the Bessel function J_n, $k_{n,m} = \sqrt{\omega_{n,m}^2 - \Omega_{n,m}^2}/c$, $\omega_{n,m}$ is the cutoff frequency of the (n,m) mode, and $\Omega_{n,m}$ is the frequency of the trapped mode. The arbitrary phase ϕ in Eqs. (19) reflects the rotational symmetry of the cylindrical waveguide. The other two components of the field, $\mathcal{E}_r^{(n,m)}$ and $\mathcal{E}_\theta^{(n,m)}$, are small compared with $\mathcal{E}_z^{(n,m)}$ in parameter $k_{n,m}b$.

Strictly speaking, Eqs. (19) give the asymptotic field expressions valid for $|z| \gg b$; however, as a matter of fact, they are also valid in the region $|z| \sim b$, as explained in Sec. II.

For the axisymmetric enlargement, the equation for $k_{n,m}$ takes the form completely analogous to Eq. (8),

$$k_{n,m} = \frac{\mu_{n,m}^2 A}{b^3} . \tag{20}$$

For the hole, an additional factor 2 appears in the equation for the $k_{n,m}$ compared with the axisymmetric case,

$$k_{n,m} = \frac{\mu_{n,m}^2 \alpha_\theta}{2\pi b^4} . \tag{21}$$

The polarization of the trapped mode is associated with the location of the hole at the wall. Choosing $\theta = 0$ at the position of the hole, the trapped mode is polarized so that $\phi = \pi/2$ in Eq. (19). It means that $\mathcal{H}_\theta^{(n,m)}$ in the trapped mode reaches the maximum value at the location of the hole in its azimuthal variation.

V. TRANSVERSE ELECTRIC TRAPPED MODES

Both small enlargements and holes can also trap TE modes in the waveguide. The derivation of the trapped TE modes is fully analogous to that of TM modes and will be briefly outlined below.

The electromagnetic field in the (n,m) TE mode is given by

$$\begin{aligned}
Z_0 H_z^{(n,m)} &= \frac{\mu'^2_{n,m}}{b^2} J_n\left(\frac{\mu'_{n,m} r}{b}\right) \\
&\quad \times \exp(\mp\kappa_{n,m} z) \sin(n\theta + \phi) , \\
E_r^{(n,m)} &= \frac{i\omega n}{cr} J_n\left(\frac{\mu'_{n,m} r}{b}\right) \\
&\quad \times \exp(\mp\kappa_{n,m} z) \cos(n\theta + \phi) , \\
E_\theta^{(n,m)} &= -\frac{i\omega\mu'_{n,m}}{cb} J'_n\left(\frac{\mu'_{n,m} r}{b}\right) \\
&\quad \times \exp(\mp\kappa_{n,m} z) \sin(n\theta + \phi) , \\
Z_0 H_r^{(n,m)} &= \mp\frac{\mu'_{n,m}\kappa_{n,m}}{b} J'_n\left(\frac{\mu'_{n,m} r}{b}\right) \\
&\quad \times \exp(\mp\kappa_{n,m} z) \sin(n\theta + \phi) , \\
Z_0 H_\theta^{(n,m)} &= \mp\frac{n\kappa_{n,m}}{r} J_n\left(\frac{\mu'_{n,m} r}{b}\right) \\
&\quad \times \exp(\mp\kappa_{n,m} z) \cos(n\theta + \phi) ,
\end{aligned} \tag{22}$$

where $\mu'_{n,m}$ is the mth root of J'_n and $\kappa_{n,m} = \sqrt{\mu'^2_{n,m}/b^2 - \omega^2/c^2}$. The asymptotic expressions for the components of the trapped mode $\mathcal{H}_z^{(n,m)}$, $\mathcal{E}_r^{(n,m)}$, $\mathcal{E}_\theta^{(n,m)}$, $\mathcal{H}_r^{(n,m)}$, and $\mathcal{H}_\theta^{(n,m)}$ are obtained from Eq. (22) by changing $\exp(\mp\kappa_{n,m} z) \to \exp(-k_{n,m}|z|)$ and putting $-\mathrm{sgn}(z)$ instead of $\mp$ in the last two equations.

With Eq. (22), the integral in Eq. (4) [where $\mathbf{E}_1, \mathbf{H}_1$ represent the field of the trapped mode, and $\mathbf{E}_2, \mathbf{H}_2$ are now the TE mode having the frequency $\Omega_{n,m}$ of the trapped mode and exponentially decaying proportional to $\exp(-k_{n,m} z)$ in the positive direction] can be easily calculated for the surface S_1, yielding

$$\frac{\pi i \Omega_{n,m} \mu'^2_{n,m} k_{n,m} (1 + \delta_{n,0})}{Z_0 c} \left(1 - \frac{n^2}{\mu'^2_{nm}}\right) J_n^2(\mu'_{n,m}) , \tag{23}$$

where $\delta_{n,0}$ is the Kronecker symbol.

For the pillbox, the contribution from the enlargement surface comes only from the term $-\int dS\mathbf{n} \cdot \mathbf{E}^{(n,m)} \times \boldsymbol{\mathcal{H}}^{(n,m)}$. For calculation of this integral we can neglect r and θ components of the magnetic field because they are small in the parameter $k_{n,m}b$. As a result, only the $E_\theta^{(n,m)}$ component of the TE mode is left and since this component vanishes at $r = b$, we have to expand the Bessel function in the small ratio $(r - b)/b$, $E_\theta^{(n,m)} \simeq -\frac{i\omega\mu'^2_{nm}}{cb^2} J''_n(\mu'_{n,m})(r - b)\sin(n\theta + \phi)$. The magnetic field $\boldsymbol{\mathcal{H}}^{(n,m)}$ at the wall of the enlargement has r and z components (the θ component can be neglected as being small in the parameter $k_{n,m}b$), so that the cross-product $\boldsymbol{\mathcal{H}}^{(n,m)} \times \mathbf{n}$ has only a θ component that can be expressed through the surface current density i_θ at the wall, $(\boldsymbol{\mathcal{H}}^{(n,m)} \times \mathbf{n})_\theta = i_\theta$. Now, let us define a z component of the magnetic moment (per unit length of the pipe circumference) induced by the trapped mode on the pillbox as $M_z = (1/2)\int i_\theta (r - b) dl$, where the integration goes along the pillbox contour in the r-z plane. This magnetic moment is proportional to the magnetic field at the pipe wall so that one can introduce the magnetic susceptibility α_z (per unit length) in the z direction, $M_z = \alpha_z H_z^{(m,n)}$. As a result, one obtains the following equation for the enlargement contribution to Eq. (4):

$$\frac{2\pi i \Omega_{n,m} \mu'^4_{n,m} k_{n,m} (1 + \delta_{n,0})}{Z_0 c b^3} \alpha_z J''_n(\mu'_{n,m}) J_n(\mu'_{n,m}) . \tag{24}$$

Together with Eq. (23) this gives the following equation for the $k_{n,m}$:

$$k_{n,m} = \frac{2\mu'^2_{n,m}\alpha_z}{b^3} . \tag{25}$$

Note here that the parameter α_z can be found using conformal mapping technique as it has been shown in Ref. [12] for the calculation of the electric polarizability.

For the hole, the calculation similar to that performed in Sec. IV gives the following result:

$$k_{n,m} = \frac{\mu'^2_{n,m}\alpha_z}{2\pi b^4 (1 + \delta_{n,0})(1 - n^2/\mu'^2_{nm})} . \tag{26}$$

VI. DISCUSSION

We have proven the existence of trapped modes in a smooth waveguide with a small discontinuity, such as an enlargement or a hole. Such discontinuities are typically present in any vacuum chamber of an accelerator. The physical mechanism of the trapping is the interaction of a mode having the frequency close to the cutoff with the magnetic moment of the discontinuity induced by the magnetic field in the mode. If the induced magnetic moment is directed along the magnetic field (the case of the enlargement and the hole), the interaction lowers the frequency of the mode below cutoff, making the mode nonpropagating. However, for a discontinuity having the magnetic moment directed against the magnetic field of the mode (such as an iris), the interaction does not bring about a trapped mode. The field in trapped modes exponentially decays away from the discontinuity on a distance large compared with the radius of the pipe.

So, with respect to the trapped modes, small enlargements or holes are very different from discontinuities that protrude into the chamber. It is interesting to compare this fact with their behavior at low frequencies, where these two kinds of discontinuities are very similar since they both produce inductive contributions to the impedance. The reason for such a difference is that the low-frequency impedance is due to both the induced magnetic and electric dipole moments, which have opposite signs. (See [12] for the case of axisymmetric discontinuities and [5] for holes.) For a chamber enlargement (e.g., a pillbox) the magnetic contribution to the impedance is larger than the electric one; for a chamber contraction (e.g., an iris) the situation is reversed, but both the moments change sign. As a result, the imaginary part of the impedance at low frequencies has a fixed sign. Unlike that, the appearance of the trapped modes is caused by the interaction with the induced magnetic moment only and depends on its sign, as explained above.

The importance of the trapped modes for accelerator physics is motivated by the fact that they can produce high and narrow peaks in the coupling impedance. The formulas derived in the present article refer to the case of a single discontinuity; however, in reality, trapped modes can interact with many discontinuities simultaneously (for example, in a liner with a regular array of pumping holes). In this case, the contribution of the trapped mode into impedance can be substantially amplified. A detailed study of this effect will be presented in a separate paper.

ACKNOWLEDGMENTS

One of the authors (S.K.) would like to thank Dr. V. I. Balbekov and Professor R. L. Gluckstern for useful discussions and remarks. The Superconducting Super Collider Laboratory is operated by the Universities Research Association, Inc., for the U.S. Department of Energy under Contract No. DE-AC35-89ER40486.

[1] H. Henke, CERN Report No. CERN-LEP-RF/85-41, 1985 (unpublished).
[2] S.S. Kurennoy and S.V. Purtov, Part. Accel. **36**, 223 (1992).
[3] S. Heifets and S. Kheifets, Rev. Mod. Phys. **63**, 631 (1991).
[4] V.I. Balbekov, Institute for High Energy Physics, Protvino, Report No. IHEP 93-55, 1993 (unpublished) (in Russian).
[5] S.S. Kurennoy, Part. Accel. **39**, 1 (1992).
[6] R.L. Gluckstern, Phys. Rev. A **46**, 1106 (1992).
[7] R.E. Collin, *Field Theory of Guided Waves* (McGraw-Hill, New York, 1960).
[8] K. Halbach and R.F. Holsinger, Part. Accel. **7**, 213 (1976).
[9] L.D. Landau and E.M. Lifshitz, *Electrodynamics of Continuous Media* (Pergamon Press, Oxford, 1960).
[10] S.S. Kurennoy, Phys. Part. Nucl. **24**, 380 (1993).
[11] H.A. Bethe, Phys. Rev. **66**, 163 (1944).
[12] S.S. Kurennoy and G.V. Stupakov, Part. Accel. (to be published).